Available online at www.sciencedirect.com
ScienceDirect
Thermochimica Acta 452 (2007) 106–115
thermochimica acta
www.elsevier.com/locate/tca

Application of model-fitting and model-free kinetics to the study of non-isothermal dehydration of equilibrium swollen poly (acrylic acid) hydrogel: Thermogravimetric analysis

B. Janković *, B. Adnađević, J. Jovanović

Faculty of Physical Chemistry, University of Belgrade, Studentski trg 12-16, P.O. Box 137, 11001 Belgrade, Serbia and Montenegro

Received 9 June 2006; received in revised form 24 July 2006; accepted 26 July 2006
Available online 2 August 2006

Abstract

The dehydration kinetics of equilibrium swollen poly (acrylic acid) hydrogel is analyzed by both model-fitting and model-free approaches. The conventional model-fitting approach assuming a fixed mechanism throughout the reaction and extract a single values of the apparent activation energy (E_a) and pre-exponential factor (A) and was found to be too simplistic. The values of Arrhenius parameters obtained in such a way are in fact an average that does not reflect changes in the reaction mechanism and kinetics with the extent of conversion. The model-free approach allows for a change of mechanism and activation energy, E_a, during the course of a reaction and is therefore more realistic. The complexity of the dehydration of poly (acrylic acid) hydrogel is illustrated by the dependence of E_a and A on the extent of conversion, α ($0.05 \leq \alpha \leq 0.98$). Under non-isothermal conditions, E_a decreases with α for $0 \leq \alpha \leq 0.50$, followed by an approximately constant value of E_a during further dehydration. For $0 \leq \alpha \leq 0.50$, dehydration is complex, which probably involving a combination of several processes. In the constant-E_a region, non-isothermal dehydration follows the three-dimensional phase boundary model (R3). The complex hydrogen-bond pattern in poly (acrylic acid) hydrogel is probably responsible for the observed dehydration behavior. An existence of compensation effect is accepted and explanation of compensation effect appearance during the hydrogel dehydration is suggested.

Keywords: Poly (acrylic acid) hydrogel; Dehydration; Model-fitting; Model-free; Apparent activation energy

1. Introduction

Hydrogels may be conveniently described as hydrophilic polymers that are swollen by, but not dissolve in water. They are three-dimensional cross-linked polymeric structures that are able to swell in the aqueous environment. Depending upon the type of the monomers incorporated into the gels, they may demonstrate a large volume transition and associated phase transition as a function of physical and chemical variables, such as temperature [1,2], pH [3,4] and ionic strength [5] as well as electric and magnetic fields [6] and thus are known as "stimuli-responsive" polymers. Although many naturally occurring polymers may be used to produce this type of materials, the structural versatility available in synthetic hydrogels has given them distinctive properties, which in turn have enhanced their practical utility. Due to characteristic properties such as swellability in water, hydrophilicity, biocompatibility and lack of toxicity, hydrogels have been utilized in a wide range of biological, medical, pharmaceutical and environmental applications [7].

The most important properties of hydrogels are their swelling capacity and swelling behavior, their mechanical properties and also dehydration behavior. These properties will be effected hydrogel usability in various applications. Although, the swelling behavior and swelling kinetics of various types of hydrogels are extensively studied [8–12], there are much lesser information concerning hydrogel mechanical properties [13,14] and according to our knowledge there are not available apparent investigations concerning the kinetics of hydrogel dehydration. The aim of this study was to investigate of non-isothermal dehydration process of poly (acrylic acid) hydrogel using model-fitting and model-free kinetic analysis.

As Vyazovkin [15,16] explains, both isothermal and non-isothermal kinetics, the currently dominating approach appears

* Corresponding author. Tel.: +381 11 187 133; fax: +381 11 187 133.
E-mail address: bojanjan@ffh.bg.ac.yu (B. Janković).

0040-6031/$ – see front matter © 2006 Elsevier B.V. All rights reserved.
doi:10.1016/j.tca.2006.07.022

to be force-fitting of experimental data to different reaction models. Following these indiscriminate model-fitting methods, Arrhenius parameters (the pre-exponential factor, A, and the activation energy, E_a) are determined by the form of $f(\alpha)$ chosen ($f(\alpha)$ is the reaction model function or conversion function). Such methods tend to fail to meet even the justifiable expectations. In a non-isothermal experiment both α and T varies simultaneously. The application of the model-fitting approach to a single heating-rate data generally fails to achieve a clean separation between the temperature dependence, $k(T)$, and the reaction model, $f(\alpha)$. As a result, almost any $f(\alpha)$ can satisfactorily fit the data at the cost of drastic variations in the Arrhenius parameters, which compensate for the difference between the assumed form of $f(\alpha)$ and the true but unknown reaction model. For this reason, the application of the model-fitting methods to single heating-rate data produces Arrhenius parameters that are highly uncertain values.

Vyazovkin [15] points out that an alternative approach to kinetic analysis is to use model-free methods that allow for evaluating Arrhenius parameters without choosing the reaction model. The best known representatives of the model-free approach are the isoconversional methods. These methods yield the effective activation energy as a function of the extent of conversion. Knowledge of the dependence E_a on α assists in both detecting multi-step processes and drawing certain mechanistic conclusions. It is sufficient to predict the reaction kinetics over a wide temperature region. He stipulates that fitting data to reaction models cannot be used as the sole means of identifying the reaction mechanisms. Note that this is equally true in the case when statistical analysis allows one to unequivocally choose a single reaction model-statistical analysis evaluates the reaction models by the goodness of fit of the data, but not by the physical sense of applying these models to the experimental data. Even if a reaction model does not have any physical meaning at all, it may well be the best fit to the experimental data.

2. Experimental

2.1. Materials and methods

Super-absorbing cross-linked poly (acrylic acid) hydrogel, which has been applied for this investigation was synthesized using the procedure based on the simultaneous radical polymerization of acrylic acid and cross-linking of the formed poly-acrylic acid, according to general procedure described in previously work [17]. For that process, acrylic acid monomer, initiators $Na_2S_2O_8$, $Na_2S_2O_5$, H_2O_2 and cross-linking agent N,N'-methylenebisacrylamide (NMBA) were used. Equilibrium swelling degree (SD_{eq}) of the used hydrogel in distilled water at 25 °C was 8500%, determined by standard method based on weight difference of dry and swollen sample [8].

2.2. Hydrogel synthesis

Hydrogel synthesis was performed in a polymerization reactor equipped with a magnetic stirrer, reflux condenser, nitrogen income and a thermometer, in a nitrogen atmosphere. Monomer solution was prepared from: 80 mL melted glacial acrylic acid dissolved in 180 mL distilled water, and 0.8 g N,N'-methylenebisacrylamide (NMBA) and 0.08 g ethylenediaminetetraacetic acid (EDTA) both dissolved in 60 mL of distilled water. This monomer solution is placed into the reactor, stirred and de-oxygenated with nitrogen gas bubbling through the solution for 60 min. Initiator stock solutions was prepared as follows: (A) 2.5 g sodium persulfate in 22.5 mL distilled water, (B) 2.5 g sodium methabisulfite in 22.5 mL distilled water and (C) hydrogen peroxide, 30%. When the requested de-oxygenation time has passed, the following amounts of the initiator solutions was added to the monomer solutions using syringes, in the order listed with stirring: 2.4 mL of (A), 10 mL of (C) and 1.2 mL of (B). Then, reaction mixture was slightly warmed up to 50 °C until happened dramatic grows of the reaction's mixture temperature (gel-point) and left following 4 h (four) at 50 °C. The obtained gel-type product was converted into the Na^+ form (60%) by neutralization with a 3% solution of Na_2CO_3. The obtained hydrogel in bulk was cut into smaller pieces, and dried in an air oven at 105 °C to constant mass. The obtained products were stored in a vacuum exiccator before use.

2.3. Thermogravimetric measurements

Thermogravimetric curves were recorded by a Du Pont thermogravimetric analyzer TGA model 9510. These analyses were performed with 25 ± 0.1 mg samples of equilibrium swollen hydrogel in platinum pans under nitrogen atmosphere at a gas flow rate of 10 mL min^{-1}. Experiments were performed at heating rates of 5, 10 and 20 K min^{-1} from ambient temperature to 623 K.

3. Kinetic studies

In thermogravimetric analysis, the extent of conversion may be defined as the ratio of actual mass loss to the total mass loss corresponding to the investigated process:

$$\alpha = \frac{m_0 - m}{m_0 - m_f} \tag{1}$$

where m, m_0 and m_f are the actual, initial and final masses of the sample, respectively. The rate of the kinetic process can be described by Eq. (2) [18]:

$$\frac{d\alpha}{dt} = k(T) f(\alpha) \tag{2}$$

where α is a extent of conversion, $k(T)$ a temperature-dependent reaction rate constant and $f(\alpha)$ is a dependent kinetic model function. There is an Arrhenius type dependence between $k(T)$ and temperature according to Eq. (3):

$$k(T) = A \exp\left(-\frac{E_a}{RT}\right) \tag{3}$$

where A is the pre-exponential factor (usually assumed to be independent of temperature), E_a the apparent activation energy, T the absolute temperature and R is the gas constant.

For non-isothermal conditions, when the temperature varies with time with a constant heating rate $\beta = dT/dt$, Eq. (2) is modified as follows:

$$\beta \frac{d\alpha}{dT} = A \exp\left(-\frac{E_a}{RT}\right) f(\alpha). \quad (4)$$

The use of Eq. (4) supposes that a kinetic triplet (E_a, A, $f(\alpha)$) describes the time evolution of a physical or chemical change. Upon integration Eq. (4) gives:

$$g(\alpha) = \int_0^\alpha \frac{d\alpha}{f(\alpha)} = \frac{A}{\beta}\int_{T_0}^{T} \exp\left(-\frac{E_a}{RT}\right) dT \approx \frac{A}{\beta}\int_0^T \exp\left(-\frac{E_a}{RT}\right) dT = \frac{AE_a}{R\beta}\int_0^x \frac{\exp(-x)}{x^2} dx = \frac{AE_a}{R\beta} p(x) \equiv \frac{A}{\beta} I(E_a, T) \quad (5)$$

where T_0 is the initial temperature, $g(\alpha)$ the integral form of the reaction model and $p(x)$ is the temperature integral, for $x = E_a/RT$, which does not have analytical solution. If T_0 is low, it may be reasonably assumed that $T_0 \to 0$, so that the lower limit of the integral on the right-hand side of Eq. (5), T_0, can be approximated to be zero.

3.1. Model-fitting approach

3.1.1. Coats and Redfern method [19,20]

For non-isothermal experiments, model-fitting involves fitting different models to α–temperature (α–T) curves and simultaneously determining E_a and A [21]. There are numerous non-isothermal model-fitting methods; one of the most popular is the Coats and Redfern method [19,20]. This method utilizes the asymptotic series expansion in approximating $p(x)$ (Eq. (5)), producing the following equation:

$$\ln\frac{g(\alpha)}{T^2} = \ln\left(\frac{AR}{\beta E_a}\left[1 - \left(\frac{2RT^*}{E_a}\right)\right]\right) - \frac{E_a}{RT} \quad (6)$$

where T^* is the mean experimental temperature.

Plotting the left-hand side (which includes the model $g(\alpha)$) of Eq. (6) versus $1/T$ gives E_a and A from the slope and intercept, respectively. The model that gives the best linear fit is selected as the model of choice. The most commonly used reaction models for solid-state processes are listed in Table 1.

3.1.2. Kennedy and Clark method [22]

The method proposed by Kennedy and Clark [22] is based on the expression:

$$T = \beta t + T_0 \quad (7)$$

where T_0 is the initial temperature (the temperature at the start of the reaction). The basic equation is

$$\frac{\beta g(\alpha)}{T - T_0} = A \exp\left(-\frac{E}{RT}\right) \quad (8)$$

and taking the logarithm of both sides of this equation gives:

$$\ln\left[\frac{\beta g(\alpha)}{T - T_0}\right] = \ln(A) - \frac{E_a}{RT}. \quad (9)$$

Plotting the left-hand side of this equation against $1/T$ should give a straight line of slope $-E_a/R$ and intercept $\ln(A)$, assuming the reaction models $g(\alpha)$ listed in Table 1. T_0 is the temperature at which the dehydration process of hydrogel starts. The experimentally determined values of T_0 at considered heating rates are: $T_0 = 293.2$ K.

3.1.3. Determination of the reaction model by masterplots method

The use of the so-called "masterplots" has received increased attention as a means for the determination of the reaction model of solid-state reactions [23]. Essentially, masterplots are reference theoretical curves depending on the reaction model but independent of the Arrhenius parameters. Since the experimental kinetic data can easily be transformed into masterplots, a comparison among the theoretical masterplots obtained by assuming different reaction models and the experimental masterplots allows the selection of the appropriate reaction model or, at least, the appropriate type of kinetic model. Application of the masterplot method for thermoanalytical data recorded under non-isothermal conditions requires previously knowledge of the activation energy. By using a reference at point $\alpha = 0.5$ and according to Eq. (5), the following equation is obtained,

$$g(0.5) = \left(\frac{AE_a}{R\beta}\right) p(x_{0.5}) \quad (10)$$

where $x_{0.5} = E_a/RT_{0.5}$ and $T_{0.5}$ is the temperature required to attain 50% conversion. When Eq. (5) is divided by Eq. (10), the following equation is obtained:

$$\frac{g(\alpha)}{g(0.5)} = \frac{p(x)}{p(x_{0.5})}. \quad (11)$$

Plotting $g(\alpha)/g(0.5)$ versus α corresponds to theoretical masterplots of various $g(\alpha)$ functions. The knowledge of temperature as a function of α and the value of E_a for the process should be known in advance to draw the experimental masterplots of $p(x)/p(x_{0.5})$ versus α from experimental data obtained at a given heating rate. To draw the experimental masterplots of $p(x)/p(x_{0.5})$ versus α from experimental data obtained under different heating rates, an approximate formula [24] of $p(x)$ with high accuracy was used $p(x) = \exp(-x)/[x(1.00198882x + 1.87391198)]$. Eq. (11) indicates that, for a given α, the experimental value of $p(x)/p(x_{0.5})$ and theoretically calculated values of $g(\alpha)/g(0.5)$ are equivalent when an appropriate reaction model is used. Consequently, this integral "model-fitting" masterplot method can be used to determine reaction models for solid-state reactions.

3.2. Model-free approach

3.2.1. Friedman (FR) method [25]

The differential isoconversional method suggested by Friedman [25] (FR method) is based on Eq. (4) in logarithmic form

Table 1
Algebraic expressions of $f(\alpha)$ and $g(\alpha)$ for the reaction models considered in the present work

No.	Symbol	Reaction model	$f(\alpha)$	$g(\alpha)$
1	P1	Power law	$4\alpha^{3/4}$	$\alpha^{1/4}$
2	P2	Power law	$3\alpha^{2/3}$	$\alpha^{1/3}$
3	P3	Power law	$2\alpha^{1/2}$	$\alpha^{1/2}$
4	P4	Power law	$2/3\alpha^{-1/2}$	$\alpha^{3/2}$
5	R1	Zero-order (Polany–Winger equation)	1	α
6	R2	Phase-boundary controlled reaction (contracting area, i.e., bidimensional shape)	$2(1-\alpha)^{1/2}$	$[1-(1-\alpha)^{1/2}]$
7	R3	Phase-boundary controlled reaction (contracting volume, i.e., tridimensional shape)	$3(1-\alpha)^{2/3}$	$[1-(1-\alpha)^{1/3}]$
8	F1	First-order (Mampel)	$(1-\alpha)$	$-\ln(1-\alpha)$
9	F3/2	Three-halves order	$(1-\alpha)^{3/2}$	$2[(1-\alpha)^{-1/2}-1]$
10	F2	Second-order	$(1-\alpha)^{2}$	$(1-\alpha)^{-1}-1$
11	F3	Third-order	$(1-\alpha)^{3}$	$(1/2)[(1-\alpha)^{-2}-1]$
12	A3/2	Avrami–Erofeev ($n=1.5$)	$(3/2)(1-\alpha)[-\ln(1-\alpha)]^{1/3}$	$[-\ln(1-\alpha)]^{2/3}$
13	A2	Avrami–Erofeev ($n=2$)	$2(1-\alpha)[-\ln(1-\alpha)]^{1/2}$	$[-\ln(1-\alpha)]^{1/2}$
14	A3	Avrami–Erofeev ($n=3$)	$3(1-\alpha)[-\ln(1-\alpha)]^{2/3}$	$[-\ln(1-\alpha)]^{1/3}$
15	A4	Avrami–Erofeev ($n=4$)	$4(1-\alpha)[-\ln(1-\alpha)]^{3/4}$	$[-\ln(1-\alpha)]^{1/4}$
16	D1	One-dimensional diffusion	$1/2\alpha$	α^{2}
17	D2	Two-dimensional diffusion (bidimensional particle shape) Valensi equation	$1/[-\ln(1-\alpha)]$	$(1-\alpha)\ln(1-\alpha)+\alpha$
18	D3	Three-dimensional diffusion (tridimensional particle shape) Jander equation	$3(1-\alpha)^{1/3}/2[(1-\alpha)^{-1/3}-1]$	$[1-(1-\alpha)^{1/3}]^{2}$
19	D4	Three-dimensional diffusion (tridimensional particle shape) Ginstling–Brounshtein	$3/2[(1-\alpha)^{-1/3}-1]$	$(1-2\alpha/3)-(1-\alpha)^{2/3}$

and leads to:

$$\ln\left[\beta_i\left(\frac{\mathrm{d}\alpha}{\mathrm{d}T}\right)_{\alpha,i}\right] = \ln[A_\alpha f(\alpha)_i] - \frac{E_{\mathrm{a},\alpha}}{RT_{\alpha,i}} \quad (12)$$

where subscripts i and α designates a given value of heating rate and extent of conversion, respectively. For α = const., the plot $\ln[\beta(\mathrm{d}\alpha/\mathrm{d}T)]$ versus $(1/T)$ should be a straight line whose slope can be used to evaluate the apparent activation energy.

3.2.2. Flynn–Wall–Ozawa (FWO) method [26,27]

The isoconversional integral method suggested independently by Flynn and Wall [26] and Ozawa [27] uses Doyle's approximation of $p(x)$ [28–30]. This method is based on the equation:

$$\log\beta = \log\frac{AE_\mathrm{a}}{Rg(\alpha)} - 2.315 - 0.4567\frac{E_\mathrm{a}}{RT}. \quad (13)$$

Thus, for α = const., the plot $\ln\beta$ versus $(1/T)$, obtained from thermograms recorded at several heating rates, should be a straight line whose slope can be used to evaluate the apparent activation energy. For $x<20$, Doyle s approximation leads to errors higher than 10%. For such cases, Flynn [31] suggested corrections in order to obtain an accurate value for the apparent activation energy.

3.2.3. Kissinger–Akahira–Sunose (KAS) method [32,33]

The Kissinger–Akahira–Sunose [32,33] method (KAS method) is based on the Coats–Redfern approximation [19] according to which, for $20<x<50$:

$$p(x) \cong \frac{\exp(-x)}{x^2}. \quad (14)$$

This is actually a particular example of a more exact approximation of the temperature integral suggested by Agrawal [34]. From relationships (5) and (14) it follows that:

$$\ln\left(\frac{\beta}{T^2}\right) = \ln\frac{AR}{E_\mathrm{a}g(\alpha)} - \frac{E_\mathrm{a}}{RT}. \quad (15)$$

Thus, for α = const., the plot $\ln(\beta/T^2)$ versus $(1/T)$ should be a straight line whose slope can be used to evaluate the apparent activation energy. The Kissinger–Akahira–Sunose method gives quite satisfactory values of E_a at $x>13$.

3.2.4. Tang (T) method [35,36]

The Tang et al. [35,36] method is based on the approximate formula [36] which introduced into Eq. (5). Taking the logarithms of both sides, Eq. (16) is obtained as:

$$\ln\left(\frac{\beta}{T^{1.894661}}\right) = \ln\left[\frac{AE_\mathrm{a}}{Rg(\alpha)}\right] + 3.635041 - 1.894661\ln E_\mathrm{a} - 1.001450\frac{E_\mathrm{a}}{RT}. \quad (16)$$

The plots of $\ln(\beta/T^{1.894661})$ versus $1/T$ give a group of straight lines. The apparent activation energy E_a can be obtained from the slope $-1.001450\,E_\mathrm{a}/R$ of the regression line.

3.2.5. Vyazovkin method [37–39]

The Vyazovkin isoconversional method [37–39] is a non-isothermal method that utilizes an accurate, non-linear, Senum–Yang [40] approximation of $p(x)$ (Eq. (5)), which leads

to,

$$\Phi = \left| \sum_{i=1}^{n} \sum_{j \neq i}^{n} \frac{I(E_{a,\alpha,}, T_{\alpha,i})\beta_j}{I(E_{a,\alpha,}, T_{\alpha,j})\beta_i} \right| \quad (17)$$

where n is the number of heating rates, $I(E_{a,\alpha},T_{\alpha,i})$ the exponential integral ($p(x)$) that results from heating rate β_i while $I(E_{a,\alpha},T_{\alpha,j})$ is the exponential integral from heating rate β_j. The 4th degree Senum–Yang approximation was chosen for our work.

The apparent activation energy (E_a) at a given extent of conversion is the value that minimizes Φ in the above equation. This non-linear procedure suggested by Vyazovkin shows extremely low errors in the activation energy, which are practically independent on x value [37]. An advantage of the advanced isoconversional method is that it can be applied to study the kinetics under arbitrary temperature programs [39]. Vyazovkin has provided a detailed description of this numerical algorithm [39,41].

4. Results and discussion

4.1. TG and DTG curves of dehydration process of poly (acrylic acid) hydrogel

The TG and DTG curves of the dehydration process of poly (acrylic acid) hydrogel samples obtained at different heating rates (5, 10 and 20 K min^{-1}) are shown in Fig. 1.

All the thermogravimetric curves are asymmetric (Fig. 1) and were moves to higher temperatures with increase in heating rate. Values of initial temperature (T_0), inflection temperature (T_p), final temperature (T_f) and the extent of reaction at maximum reaction rate α_{max}, at various heating rates are presented in Table 2.

Increasing of heating rate leads to increase of the characteristic temperatures values (temperatures T_p and T_f) on the obtained thermogravimetric curves. The values of α_{max} at 5 and 10 K min^{-1} are equal, while the value of α_{max} at 20 K min^{-1} is a little higher. On the DTG curves one well-defined peak can be distinguished. On the DTG curve at 20 K min^{-1}, one mildly shoulder was discerned at $T = 363.2$ K. With heating rate increase, the maximums on DTG curves moves to higher temperatures and peaks become more widen.

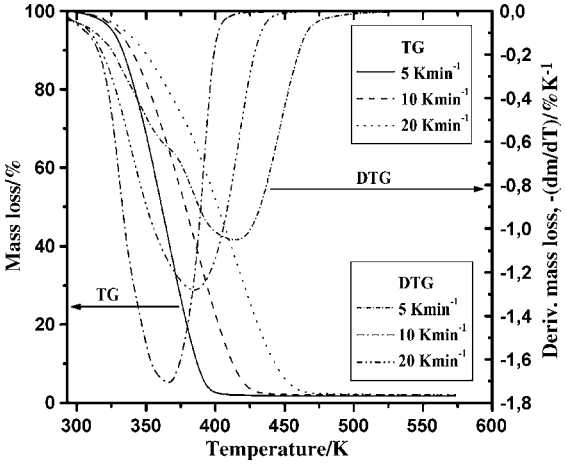

Fig. 1. TG and DTG curves of the dehydration of equilibrated swollen poly (acrylic acid) hydrogel in nitrogen atmosphere at different heating rates.

Table 2
Values of T_0, T_p, T_f and α_{max} for dehydration of poly (acrylic acid) hydrogel determined by thermogravimetric analysis at different heating rates

β (K min^{-1})	T_0 (K)	T_p (K)	T_f (K)	α_{max}
5	293.2	368.2	433.2	0.670
10	293.2	387.2	463.2	0.670
20	293.2	417.2	523.2	0.675

4.2. Model-free analysis

The non-isothermal dehydration kinetics of poly (acrylic acid) hydrogel was first analyzed by model-free methods. Starting from Eq. (1) and applying above mentioned isoconversional methods, the curves E_a versus α were obtained. The results obtained by means of FWO method were corrected according to the procedure suggested by Flynn [31].

Fig. 2 shows the variation of the apparent activation energy, E_a, as a function of the extent of conversion α, for dehydration of poly (acrylic acid) hydrogel.

From Fig. 2 one can notice the same shapes of the curves E_a versus α corresponding to the isoconversional methods. All curves shows that E_a decreases with extent of conversion (α). E_a rapidly decreases in conversion range of $0.05 \leq \alpha \leq 0.50$, and after this range ($\alpha \geq 0.50$), decreasing of E_a with α is continue approximately linearly. Generally, on the observed E_a versus α curves, two different regions are exist. First, with faster decreasing of E_a ($\alpha \leq 0.50$) and second, with slower decreasing of E_a ($\alpha \geq 0.50$), when α increasing. It was pointed out [42–44] that when E_a changes with α, the FWO, KAS, T and non-linear (V) isoconversional methods lead to close values of E_a, but which differ substantially from the values of E_a obtained using the iso-

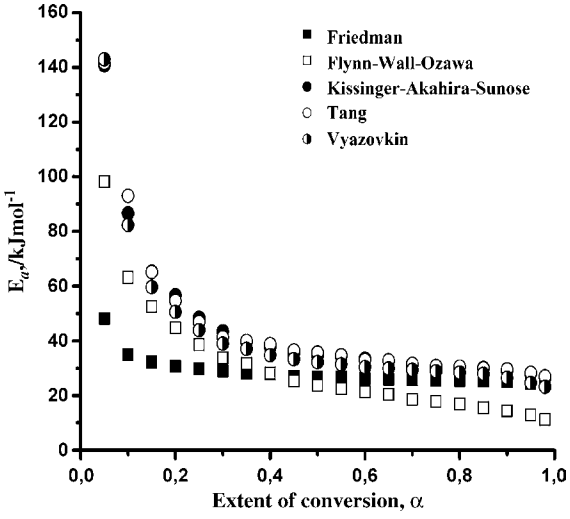

Fig. 2. The activation energy, E_a, plotted as a function of the extent of conversion, α, for the dehydration of poly (acrylic acid) hydrogel under non-isothermal conditions.

conversional method suggested by Friedman. These differences could be due to the approximation of the temperature integral that were used in the derivations of the relations that ground FWO, KAS, *T* and non-linear methods. Therefore, we think that the existence of significant differences between the apparent activation energy calculated by Friedman (average value $E_a = 28.5\,kJ\,mol^{-1}$) and values of E_a calculated using the others isoconversional methods (average values are $E_a = 30.6, 44.7, 45.1$ and $41.8\,kJ\,mol^{-1}$ for FWO, KAS, *T* and *V*, respectively) (see Fig. 2) are due to the way in which the relations that form the basis of the "integral" methods are derived. All applied isoconversional methods do not suggest a direct way of evaluating either the pre-exponential factor (*A*) or the analytical form of the reaction model ($f(\alpha)$), for the investigated dehydration process of equilibrium swollen poly (acrylic acid) hydrogel.

Furthermore, the obtained results reveal that the dependence of the apparent activation energy (E_a) on the extent of conversion (a) helps not only to disclose the complexity of a dehydration hydrogel process, but also to identify its kinetic scheme.

The curves obtained in this paper (Fig. 2), reveal a typical dependence for reversible reactions according to Vyazovkin et al [45–48]. Vyazovkin and Linert [46] have shown that the decreasing dependence of E_a on α corresponds to the kinetic scheme of an endothermic reversible reaction followed by an irreversible one. For such a process E_a is limited by the sum of the activation energy of the irreversible reaction and the enthalpy of the reversible reaction at low conversions. At high values of conversions, E_a is limited only by the activation energy of the irreversible reaction at high α [46]. An examples of such reversible reactions can be the dehydration of crystal hydrates, such as calcium oxalate monohydrate [45] and thermal decomposition of tetrazole [47], which displays these type of dependencies of E_a on α (Fig. 2). In our case, the dehydration process of hydrogel probably proceeding through the endothermic stage at low extent of conversions (to the values of $\alpha \approx 0.45$), which is characterised by a high value of the apparent activation energy (from 48.2 to $27.0\,kJ\,mol^{-1}$ for Friedman method or from 143.0 to $33.3\,kJ\,mol^{-1}$ for Vyazovkin method). This high value of the *effective* activation energy represents the sum of the enthalpy of the reversible process and of the apparent activation energy of the irreversible process. On the other hand, very low values (less than $26.7\,kJ\,mol^{-1}$—see Fig. 2) of E_a at higher conversions are characteristic of the process proceeding through a reversible exothermal stage. In the conversion range from $\alpha = 0.50$ to $\alpha = 0.95$, the apparent activation energy is approximately independent of the extent of conversion, which is indicative of the single-stage character of the irreversible process. On that way, in the region of Fig. 2 in which E_a is nearly constant, the dehydration reaction can be assumed to follow a single-step reaction under the respective heating condition, and the data can be model fitted to reveal the dehydration mechanism. Frequently the rate parameters ($d\alpha/dT$, E_a and *A*), measured for dehydration, are sensible to the availability of water vapor in the vicinity of the reactant [18]. This is one of the fundamental factors for the apparent variation in the kinetic data, sometimes found between different reports concerning the some reaction. The decrement, as well as the approximately constant value of E_a against α (around $25.7\,kJ\,mol^{-1}$ calculated by FR method and $28.9\,kJ\,mol^{-1}$ calculated by Vyazovkin method), demonstrate the importance of the continuous flow of nitrogen to guarantee a slow water vapor pressure and then favor the direct irreversible reaction.

4.3. Model-fitting analysis

After model-free analysis has been performed, model fitting can be performed in the conversion region where the apparent activation energy is approximately constant, and where a single model may fit. Model-fitting analysis is preferably conducted after model-free analysis unless there are good reasons to believe that the reaction proceeds via a single mechanism. The non-isothermal kinetic data of hydrogel dehydration at $0.50 \leq \alpha \leq 0.95$, where model-free analysis indicates approximately constant activation energy, were then fitted to each of the 19 reaction models listed in Table 1. The values of activation energies (E_a), pre-exponential factors (ln A) and the coefficients of linear correlations (*r*) for three kinetic models which described dehydration process of poly (acrylic acid) hydrogel very well at all constant heating rates (5, 10 and $20\,K\,min^{-1}$) are presented in Table 3.

As shown in Table 3, for both applied methods (Coats–Redfern and Kennedy–Clark methods), the Arrhenius parameters (E_a, $\ln A$) for hydrogel dehydration process are highly

Table 3
Arrhenius parameters determined by Coats–Redfern and Kennedy–Clark methods (model-fitting), for three kinetic models which best describe the investigated dehydration process ($0.50 \leq \alpha \leq 0.95$)

$5\,K\,min^{-1}$				$10\,K\,min^{-1}$				$20\,K\,min^{-1}$			
Model[a]	ln *A*	E_a ($kJ\,mol^{-1}$)	$\lvert r\rvert$	Model[a]	ln *A*	E_a ($kJ\,mol^{-1}$)	$\lvert r\rvert$	Model[a]	ln *A*	E_a ($kJ\,mol^{-1}$)	$\lvert r\rvert$
CR method											
7	9.66	38.9	0.9998	6	6.11	27.6	0.9988	6	5.19	24.7	0.9994
8	14.39	48.8	0.9991	7	7.24	31.8	0.9999	7	6.29	29.0	0.9999
18	23.87	83.9	0.9998	18	18.67	70.2	0.9999	18	16.34	65.1	1.0000
KC method											
7	5.88	30.2	0.9999	6	3.38	21.2	0.9991	6	3.15	20.2	0.9996
8	10.38	40.1	0.9994	7	4.37	25.4	1.0000	7	4.09	24.5	0.9998
18	19.31	75.2	0.9999	18	15.01	63.7	1.0000	18	13.33	60.6	0.9999

[a] Enumeration of the models is given in Table 1.

variable, exhibiting a strong dependence on the reaction model chosen. On the other hand, two different models, R3 (three-dimensional phase boundary) and D3 (three-dimensional diffusion (Jander)), give a highest coefficients of linear correlations at all heating rates. However, the analysis of the corresponding residual plots, applied for both models in Table 3, shows that only model R3 gives a pattern close to the ideal randomness. Therefore, model R3 provides a good description of the non-isothermal dehydration kinetics over this range of the conversion. Also, according to Table 3, it could be found that the E_a values of hydrogel dehydration in N_2 corresponding to the reaction model R3 have best agreement with the values obtained by isoconversional methods (Fig. 2).

The Arrhenius parameters of hydrogel dehydration, can be calculated for the overall process at given heating rate, from Eq. (12) after rearrangement [49],

$$\ln\left[\frac{\beta(\mathrm{d}\alpha/\mathrm{d}T)}{f_j(\alpha)}\right] = \ln A_j - \frac{E_{a,j}}{RT} \tag{18}$$

where $f_j(\alpha)$ is differential form of jth reaction model (Table 1), $\ln A_j$ and $E_{a,j}$ are the pairs of Arrhenius parameters obtained for jth reaction model. Varying the different $f_j(\alpha)$ models, from Eq. (18) for the best chosen reaction model (Table 1), the Arrhenius parameters ($\ln A_j$, $E_{a,j}$) of the investigated process were calculated. Table 4 shows the calculated Arrhenius parameters for reaction models which best described the dehydration process of poly (acrylic acid) hydrogel at every heating rate, in the conversion range of $0.10 \le \alpha \le 0.98$.

From Table 4, it can be seen that the reaction model R3, at heating rates of 5 and 10 K min^{-1} is the best model for describing the hydrogel dehydration process, in conversion range of $0.10 \le \alpha \le 0.98$. The obtained values of apparent activation energies (E_a) for this reaction model, are in good agreement with values of E_a obtained by different isoconversional methods for $\alpha > 0.5$ (Fig. 2). However, at heating rate of 20 K min^{-1}, the three-dimensional diffusion (Jander) (D3) was the best reaction model for hydrogel dehydration process. The obtained value of apparent activation energy is in a good agreement with values of apparent activation energies obtained by isoconversional methods at low values of α (see also Fig. 2).

Fig. 3 shows the experimental masterplots of $p(x)/p(x_{0.5})$ against α constructed from experimental data under different heating rates. The theoretical masterplots corresponding to the $g(\alpha)$ functions for R2, R3 and D3 models (Table 1) are also shown in Fig. 3.

It is shown that the all experimental masterplots of dehydration process at 5, 10 and 20 K min^{-1} are conformabled with

Table 4
Arrhenius parameters ($\ln A$, E_a) of non-isothermal dehydration of poly (acrylic acid) hydrogel obtained by Eq. (18) and corresponding best fit reaction models (for $0.10 \le \alpha \le 0.98$)

β (K min^{-1})	Model	$\ln A$	E_a (kJ mol^{-1})	$\lvert r\rvert$
5	R3	8.01	33.3	0.9984
10	R3	6.34	28.3	0.9994
20	D3	16.00	63.7	0.9997

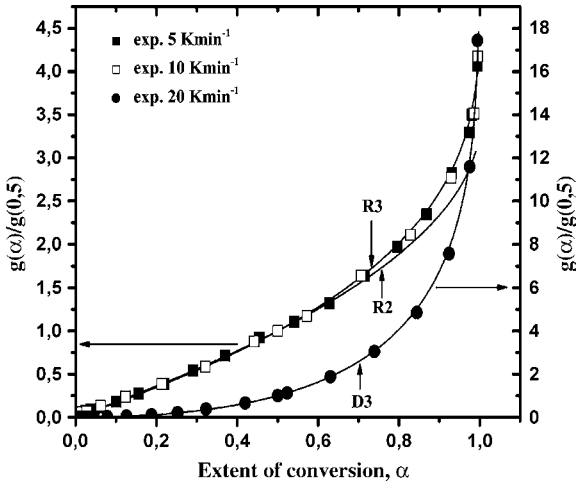

Fig. 3. Masterplots of theoretical $g(\alpha)/g(0.5)$ vs. α for R2, R3 and D3 theoretical reaction models and experimental masterplots for the dehydration of poly (acrylic acid) hydrogel at a heating rates of 5, 10 and 20 K min^{-1}.

theoretical masterplots for the corresponding reaction models. The comparison of the experimental masterplots with theoretical ones indicates that the kinetic process for the dehydration of poly (acrylic acid) hydrogel can be most probably described by R3 model, at lower (5 K min^{-1}) and middler (10 K min^{-1}) heating rates, β. At highest value of heating rate ($\beta = 20$ K min^{-1}), the dehydration process of poly (acrylic acid) hydrogel follow the three-dimensional diffusion (D3) reaction model. It is likely that the apparent mechanism of overall reaction cannot be expressed in terms of one simple reaction model.

4.4. Numerical reconstruction of the experimental kinetic function

Model-free analysis, as well as providing E_a as a function of α, allows the experimental reaction model, $f(\alpha)$, to be reconstructed from the model-free activation energy, E_a and the pre-exponential factor, A. Comparison of the numerically reconstructed kinetic function with those of the theoretical models can provide a much clearer picture of the reaction mechanism. Use of the so-called artificial isokinetic relationship (IKR) that occurs on fitting various reaction models to the same set of non-isothermal kinetic data [50,51] can be used to evaluated A. In our case, the compensation effect (or the "θ rule") [52–55],

$$\ln A_j = a + bE_{a,j} \tag{19}$$

was observed for investigated system. In Eq. (19), subscript j refers to one of the possible models $f_j(\alpha)$ assumed to describe the process. Eq. (19) represent the artificial isokinetic relationship (IKR). The parameters of Eq. (19) are $a = \ln k_{iso}$ (an artificial isokinetic rate constant) and $b = 1/RT_{iso}$ (R is the gas constant and T_{iso} an artificial isokinetic temperature). Figs. 4 and 5 shows the artificial isokinetic relationships for dehydration process of poly (acrylic acid) hydrogel, obtained by different model-fitting methods (CR and KC methods).

The values of a, b, k_{iso} and T_{iso} of Eq. (19) obtained by different model-fitting methods for dehydration of poly (acrylic acid)

Table 5
The values of a, b, k_{iso} and T_{iso} of Eq. (19) obtained by different model-fitting methods for dehydration of poly (acrylic acid) hydrogel (for $0.50 \leq \alpha \leq 0.95$)

β (K min^{-1})	a (min$^{-1)}$	b (mol kJ^{-1})	k_{iso} (min^{-1})	T_{iso} (K)	r
CR method					
5	−3.8473	0.3549	0.0213	338.9	0.9969
10	−3.6805	0.3474	0.0252	346.3	0.9957
20	−3.2120	0.3296	0.0403	364.9	0.9954
KC method					
5	−4.1726	0.3400	0.0154	353.8	0.9920
10	−3.7100	0.3267	0.0245	368.2	0.9918
20	−3.1764	0.3065	0.0417	392.5	0.9930

hydrogel (in conversion range of $0.50 \leq \alpha \leq 0.95$) are given in Table 5.

With increasing of heating rate (β), the values of isokinetic parameters (k_{iso} and T_{iso}) also increasing. The values of artificial isokinetic temperatures obtained by KC method are higher than values of T_{iso} obtained by CR method (Table 5). If the $f(\alpha)$ model is not properly taken the isokinetic temperature may lie out of the region of the experimental temperatures [50]. From Table 5, it can be seen that the isokinetic temperatures (T_{iso}) lying in the region of the experimental temperatures and this indicated that the reaction model $f(\alpha)$ for conversions $\alpha \geq 0.50$ was a properly chosen.

Table 6 shows the obtained results for correlation parameters a and b, as well as the T_{iso} values determined from slope b of IKRs, for the best two reaction models in Table 3 (for Coats–Redfern method).

Although some models exhibit IKRs, the model considered that the best one describing the dehydration of poly (acrylic acid) hydrogel is the three-dimensional phase boundary (R3), because this model shows the best linear regression ($r = 1.0000$) and has a T_{iso} value in the region of the experimental temperatures ($T_{iso} = 353.2$ K) with what confirm the above statement.

Once the correlation parameters a and b have been evaluated, the $E_{a,\alpha}$ values are substituted for $E_{a,j}$ in Eq. (19) to estimate

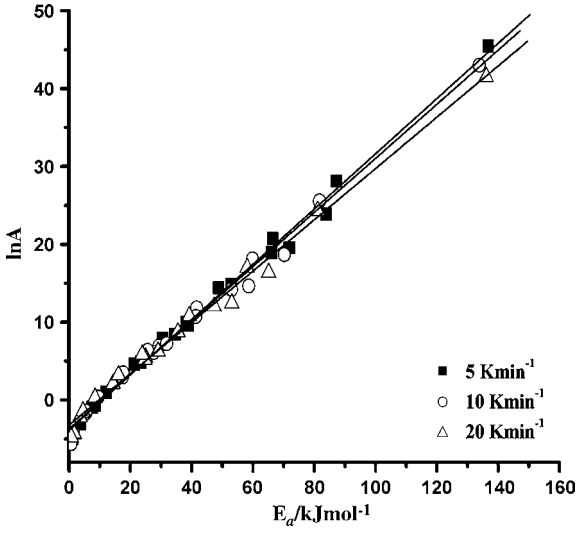

Fig. 4. The isokinetic relationships ($\ln A$ vs. E_a) obtained for the dehydration of poly (acrylic acid) hydrogel using Coats–Redfern method at different heating rates.

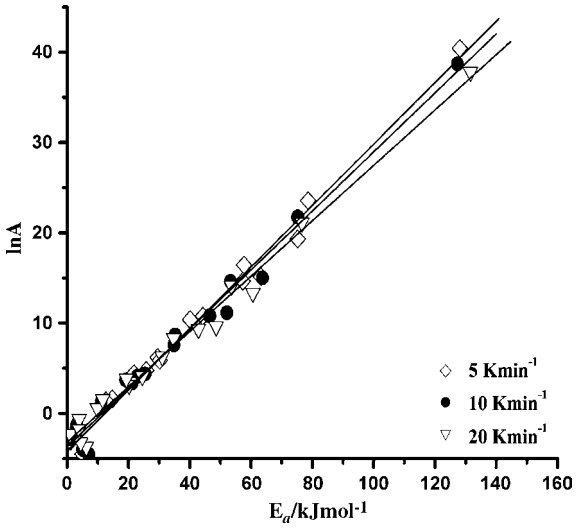

Fig. 5. The isokinetic relationships ($\ln A$ vs. E_a) obtained for the dehydration of poly (acrylic acid) hydrogel using Kennedy–Clark method at different heating rates.

the corresponding $\ln A_a$ values and obtaining the dependence of $\ln A_a$ on α. Originally, this procedure was proposed [56] for estimating the pre-exponential factor in the isoconversional method as applied to a single-step process. However, the above procedure can be applied to isolate the $\ln A_a$ on α dependence for multi-step processes [50]. Fig. 6 shows the variation of the $\ln A_a$ as a function of the extent of conversion α, which was obtained by three different isoconversional methods, for dehydration process of poly (acrylic acid) hydrogel.

From Fig. 6, it can be seen that the $\ln A_a$ shows the same dependence on a as the apparent activation energies (E_a) in Fig. 2.

Having determined values of the pre-exponential factor and the activation energy, one can reconstruct the reaction model numerically. The $f(\alpha)$ function reconstructed from the experimental data for $\alpha \geq 0.5$ at 10 K min^{-1} is plotted in Fig. 7, with

Table 6
The obtained results of isokinetic parameters for the best two reaction models in Table 3 (Coats–Redfern method)

Model[a]	a (min^{-1})	b (mol kJ^{-1})	T_{iso} (K)	r
7	−3.5856	0.3405	353.2	1.0000
18	−9.3206	0.3962	303.6	0.9991

[a] Enumeration of the models is given in Table 1.

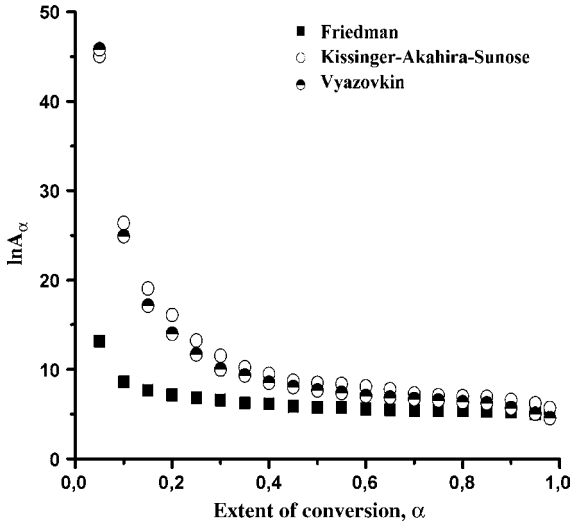

Fig. 6. Dependence of the $\ln A_\alpha$ on extent of conversion, α, for the dehydration of poly (acrylic acid) hydrogel estimated from Eq. (19) for three different isoconversional methods.

the solid lines that represent $f(\alpha)$ calculated according to the models in Table 1. Because $f(\alpha)$ depends only on α for a given model (Table 1), the construction of these solid lines does not require knowledge of E_a or A. Each line is constructed from knowledge of the individual kinetic function itself.

It is shown that the reconstructed $f(\alpha)$ function from the experimental data at $\beta = 10\,\mathrm{K\,min^{-1}}$, correspond to the $f(\alpha)$ function for reaction model R3.

Thus, on based of the obtained results, the observed dehydration behavior of the poly (acrylic acid) hydrogel is attributed to the complicated hydrogen-bond network between molecules of water and hydrogel. From the dependences of the apparent activation energy and pre-exponential factor on the α value, it was identified the existence of two regions for E_a and A_α values: The first for $\alpha \leq 0.5$, where the values of E_a and A_α decreases monotonously, and a second one for $\alpha \geq 0.5$ with the values of E_a and A_α which remains approximately constant. This constitutes a clear indication that the kinetic description of mass loss can be accomplished through at least two different mechanisms, and this conclusion is consistent with the appearance of a shoulder in DTG curves (at highest heating rate ($20\,\mathrm{K\,min^{-1}}$)). High values of apparent activation energies in the first region, can be attributed the interruptions of hydrogen bonds between molecules of water and hydrogel active centers and most probably the diffusion of water molecules through the hydrogel matrix (endothermic reaction). However, in this region ($0 \leq \alpha \leq 0.50$), hydrogel dehydration is complex, likely involving a combination of several processes. In the second region, the mechanism of hydrogel dehydration was changed, so that the rate-limiting step become the velocity of three-dimensional spherical shrinkage of the reaction interface (R3). If we make an assumption, that the conversion and the reaction model represent factors on the process which leads to the changes in Arrhenius parameters, while the pre-exponential factor is proportional to the mass concentration of the desorption centers and apparent activation energy is proportional to the energetically barrier of the observed process, it can be proposed that with the increase of the extent of conversion (α) comes to the energetic redistribution of the desorption centers. The increase of the extent of conversion (reaction progress) leads to the decrease of the number of active desorption centers per mass unit (decrease of $\ln A_a$) and to the decrease of the energy of the desorption centers (decrease of E_a), which has as a consequence changes of the Arrhenius parameters of the investigated process and appearance of the compensation effect.

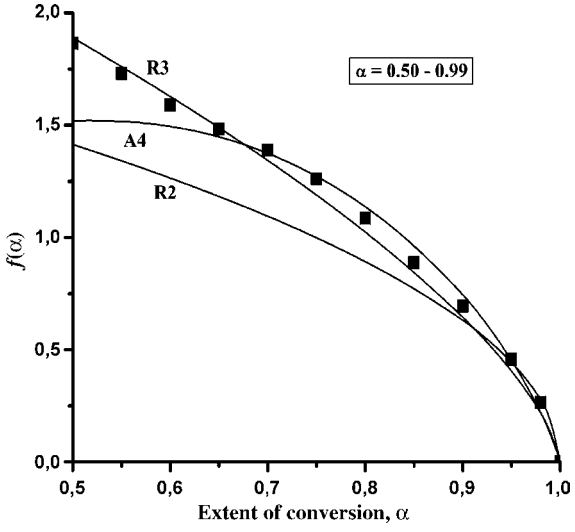

Fig. 7. The experimental kinetic function, $f(\alpha)$, reconstructed from model-free analysis of the dehydration of poly (acrylic acid) hydrogel under non-isothermal conditions (■) for $\alpha \geq 0.50$ ($\beta = 10\,\mathrm{K\,min^{-1}}$). The solid lines represent kinetic functions calculated from relevant theoretical models in Table 1.

5. Conclusions

The dehydration kinetics of poly (acrylic acid) hydrogel under non-isothermal conditions is analyzed by the model-fitting and model-free approaches. For $0 \leq \alpha \leq 0.50$, dehydration under considered conditions is complex, which probably involving a combination of several processes. One of this processes probably involve the diffusion of water molecules which is submit to the three-dimensional diffusion (Jander) mechanism (model D3). The approximately constant-E_a region of non-isothermal dehydration follows three-dimensional phase boundary (R3) kinetics. The obtained values of Arrhenius parameters (for R3 reaction model) by model-fitting methods in conversion range of $0.50 \leq \alpha \leq 0.95$ are in good agreement with values of E_a and $\ln A$ obtained by different isoconversional methods. The obtained artificial isokinetic temperatures (T_{iso}) at different heating rates of the system, were lying in the region of the experimental temperatures and this indicated that the reaction model $f(\alpha)$ for conversions $\alpha \geq 0.50$ was a properly chosen. The appearances of the compensation effect is explained by changes of energetic distribution of the active desorption centers.

Acknowledgment

The investigation was partially supported by the Ministry of Science and Environmental Protection of Serbia, under the Project 142025.

References

[1] A.S. Hoffman, J. Control. Rel. 6 (1987) 297.
[2] W.F. Lee, C.H. Shieh, J. Appl. Polym. Sci. 71 (1999) 221.
[3] E.O. Akala, P. Kopeckova, J. Kopecek, Biomaterials 19 (1998) 1037.
[4] E. Hirokawa, T. Tanaka, J. Chem. Phys. 81 (1984) 6379.
[5] R.A. Siegel, B.A. Firestone, Macromolecules 1 (1988) 3254.
[6] S.R. Eisenberg, A.J. Grodzinski, J. Membr. Sci. 19 (1984) 173.
[7] N.A. Peppas, Hydrogels in Medicine and Pharmacy, Vol 1: Fundamentals, CRC, Boca Raton, FL, 1986.
[8] E. Karadağ, D. Saraydin, Polym. Bull. 48 (2002) 299.
[9] D. Saraydin, Y. Caldiran, Polym. Bull. 46 (2001) 91.
[10] I. Katime, J.L. Velada, R. Novoa, E. Diaz de Apodaca, J. Puig, E. Mendizabal, Polym. Int. 40 (1996) 281.
[11] E. Keradağ, D. Saraydin, Turk. J. Chem. 26 (2002) 863.
[12] P.M. de la Torre, S. Torrado, S. Torrado, Biomaterials 24 (2003) 1459.
[13] C.M.A. Lopes, M.I. Felisberti, Biomaterials 24 (2003) 1279.
[14] J. Hao, Y. Liu, S. Zhou, Z. Li, X. Deng, Biomaterials 24 (2003) 1531.
[15] S. Vyazovkin, Thermochim. Acta 355 (2000) 155.
[16] S. Vyazovkin, C.A. Wight, Thermochim. Acta 340–341 (1999) 53.
[17] J. Jovanović, B. Adnadević, XLI Consultation of Serbian Chemical Society, SSHD, Belgrade, 23–24 January, Book of Abstracts, vol. HM13, 2003, p. 119.
[18] M.E. Brown, D. Dollimore, A.K. Galwey, Reactions in the Solid State. Comprehensive Chemical Kinetics, vol. 22, Elsevier, Amsterdam, 1980.
[19] A.W. Coats, J.P. Redfern, Nature. 201 (1964) 68.
[20] A.W. Coats, J.P. Redfern, J. Polym. Sci. Part B: Polym. Lett. 3 (1965) 917.
[21] S. Vyazovkin, C.A. Wight, J. Phys. Chem. A 101 (1997) 8279.
[22] J.A. Kennedy, S.M. Clark, Thermochim. Acta 307 (1997) 27.
[23] F.J. Gotor, J.M. Criado, J. Malek, M. Koga, J. Phys. Chem. A 104 (2000) 10777.
[24] T. Wanjun, L. Yuwen, Z. Hen, W. Zhiyong, W. Cunxin, J. Therm. Anal. Cal. 74 (2003) 309.
[25] H.L. Friedman, J. Polym. Sci. C 6 (1963) 183.
[26] J.H. Flynn, L.A. Wall, J. Res. Natl. Bur. Stand. Sect. A 70 (1966) 487.
[27] T. Ozawa, Bull. Chem. Soc. Japan 38 (1965) 1881.
[28] C.D. Doyle, Anal. Chem. 33 (1961) 77.
[29] C.D. Doyle, J. Appl. Polym. Sci. 5 (1961) 285.
[30] C.D. Doyle, Nature 207 (1965) 290.
[31] J.H. Flynn, J. Therm. Anal. 27 (1983) 95.
[32] H.E. Kissinger, Anal. Chem. 29 (1957) 1702.
[33] T. Akahira, T. Sunose, Res. Rep. Chiba Inst. Technol. 16 (1971) 22.
[34] P.K. Agrawal, Thermochim. Acta 203 (1992) 93.
[35] T. Wanjun, L. Yuwen, Z. Hen, W. Cunxin, Thermochim. Acta 408 (2003) 39.
[36] T. Wanjun, C. Donghua, W. Cunxin, AIChE J. 52 (2006) 2211.
[37] S. Vyazovkin, D. Dollimore, J. Chem. Inform. Comp. Sci. 36 (1996) 42.
[38] S. Vyazovkin, J. Therm. Anal. 49 (1997) 1493.
[39] S. Vyazovkin, J. Comput. Chem. 18 (1997) 393.
[40] G.I. Senum, R.T. Yang, J. Therm. Anal. 11 (1977) 445.
[41] S. Vyazovkin, J. Comput. Chem. 22 (2001) 178.
[42] P. Budrugeac, A.L. Petre, E. Segal, J. Comput. Chem. 47 (1996) 123.
[43] N. Sbirrazuoli, Y. Girault, E. Elegant, Thermochim. Acta 293 (1997) 25.
[44] P. Budrugeac, D. Homentcovschi, E. Segal, J. Therm. Anal. Cal. 66 (2001) 557.
[45] S. Vyazovkin, C.A. Wight, Annu. Rev. Phys. Chem. 48 (1997) 125.
[46] S. Vyazovkin, W. Linert, Int. J. Chem. Kinet. 27 (1995) 73.
[47] S.V. Vyazovkin, A.I. Lesnikovich, V.A. Lyutsko, Thermochim. Acta 165 (1990) 17.
[48] S.V. Vyazovkin, A.I. Lesnikovich, Thermochim. Acta 165 (1990) 273.
[49] S. Vyazovkin, W. Linert, J. Solid State Chem. 114 (1995) 392.
[50] S. Vyazovkin, W. Linert, Chem. Phys. 193 (1995) 109.
[51] S. Vyazovkin, Int. J. Chem. Kinet. 28 (1996) 95.
[52] R.K. Agrawal, J. Therm. Anal. 31 (1986) 73.
[53] R.K. Agrawal, J. Therm. Anal. 35 (1989) 909.
[54] S.V. Vyazovkin, A.J. Lesnikovich, I.S. Romanovsky, J. Therm. Anal. 34 (1988) 609.
[55] D. Klinar, J. Golob, M. Krajnc, Acta Chim. Slov. 50 (2003) 473.
[56] S.V. Vyazovkin, A.I. Lesnikovich, Thermochim. Acta 128 (1988) 297.